

Black Hole Criticality in the Brans-Dicke Model

Steven L. Liebling and Matthew W. Choptuik

Center for Relativity, The University of Texas, Austin, TX 78712-1081

(May 5, 2022)

We study the collapse of a free scalar field in the Brans-Dicke model of gravity. At the critical point of black hole formation, the model admits two distinctive solutions dependent on the value of the coupling parameter. We find one solution to be discretely self-similar and the other to exhibit continuous self-similarity.

Studies of black hole formation from the gravitational collapse of a massless scalar field have revealed interesting nonlinear phenomena at the threshold of black hole formation [1,2]. These studies have shown that Einstein's field equations possess solutions which occur precisely at the black hole threshold and which are universal with respect to the initial conditions of the evolution. More specifically, for any type of initial field configuration whose energy is parameterized by some parameter, p , the critical solution occurs at a value of $p = p^*$ such that for all $p < p^*$ no black hole is formed, and for all $p > p^*$ a black hole is necessarily formed. This critical solution, whether obtained with an initial pulse shape such as tanh or a Gaussian pulse, is identical, erasing all detail of the initial field configuration.

Though universal with respect to initial conditions, the critical solution is dependent on the specific matter model involved. In the case of a real scalar field [1], a discretely self-similar solution (DSS) is found, characterized by an echoing exponent Δ . In other words, were an observer to take a snap-shot of the solution at some time t , he would find the same picture as when he zoomed in to a spatial scale $\exp(\Delta)$ smaller than the original at a time $t + \exp(\Delta)$ later.

In contrast to this DSS solution, other researchers, working in an axion/dilaton model, have found that the equations possess a continuously self-similar (CSS) solution [2]. Because they found this solution by assuming continuous self-similarity and solving the appropriate ordinary differential equations, they could not show whether this CSS solution is indeed a critical solution.

We find that a free real scalar field coupled to Brans-Dicke gravity contains two distinct dynamic critical solutions. As a special case, the model includes the real scalar field in general relativity and recovers the DSS solution as in [1]. Further, this model is sufficiently general that it contains the model studied in [2] as another special case. For this case, we find that the CSS solution is an attracting critical solution. Hence we present the

novel result that for a single matter model, adjustment of a coupling parameter transitions between two unique, dynamic, attracting critical solutions. Because these two solutions are both dynamic, the model is quite different from the Yang Mills model studied in [3].

Subsequent to our study, Hirschmann and Eardley, working in an even more general model, the non-linear sigma model, which includes ours, carry-out a perturbation analysis and confirm a change in stability near the value we find for the transition coupling parameter [4]. Further, from the eigenvalues of the unstable modes, they have been able to compute mass-scaling exponents. Their results concur with those we find from our numerical evolutions.

We work in spherical symmetry with the metric

$$ds^2 = -\alpha(r, t)^2 dt^2 + a(r, t)^2 dr^2 + r^2 d\Omega^2, \quad (1)$$

where $\alpha(r, t)$ represents the lapse function in the 3+1 formalism and r measures proper surface area.

The Brans-Dicke model is described by the field equations

$$G_{\mu\nu} = \frac{8\pi}{\phi(r, t)} T_{\mu\nu}^{\text{total}} \quad (2)$$

where $1/\phi(r, t)$ represents the freedom of the conventional gravitational constant to vary [5]. The total stress-energy tensor consists of two terms

$$T^{\text{total}} = T^{\text{matter}} + T^{\text{BD}}, \quad (3)$$

where T^{BD} represents the energy associated with the Brans-Dicke field ϕ and T^{matter} is the conventional tensor associated with matter sources [5]. For this study our sole matter source is a free massless minimally coupled scalar field $\psi(r, t)$ governed by

$$\square\psi = 0 \quad (4)$$

and whose associated stress-energy is

$$T_{\mu\nu}^{\text{matter}} = \psi_{,\mu}\psi_{,\nu} - \frac{1}{2}g_{\mu\nu}\psi^{,\rho}\psi_{,\rho}. \quad (5)$$

The Brans-Dicke field satisfies the generally covariant wave equation

$$\square\phi = 4\pi\lambda T^{\text{matter}} \quad (6)$$

where λ , a constant, represents the strength of the coupling between the Brans-Dicke field and matter [6]. Its associated stress-energy tensor is

$$T_{\mu\nu}^{\phi} = \frac{\omega}{8\pi\phi} \left(\phi_{,\mu}\phi_{,\nu} - \frac{1}{2}g_{\mu\nu}\phi_{,\rho}\phi^{,\rho} \right) + \frac{1}{8\pi} (\phi_{,\mu\nu} - g_{\mu\nu}\square\phi) \quad (7)$$

where

$$\lambda \equiv \frac{2}{2\omega + 3}. \quad (8)$$

The equations described above are said to be in the *Brans-Dicke frame* where masses are constant but inertial forces depend on the distribution of mass in the universe. However, it is possible to transform to a conformal frame in which the geometry is described by Einstein's field equations with vanishing second derivatives of ϕ . In this frame, the *Einstein frame*, masses vary with time, but the gravitational constant is indeed constant.

We achieve this conformal transformation via

$$\begin{aligned} e^{\xi} &\equiv \phi \\ g_{\mu\nu} &\rightarrow e^{\xi}g_{\mu\nu} \\ g^{\mu\nu} &\rightarrow e^{-\xi}g^{\mu\nu} \end{aligned} \quad (9)$$

after which we have the equations (now expressed in the Einstein frame)

$$T^{\text{BD}} = \left(\frac{3+2\omega}{16\pi} \right) \left(\xi_{,\mu}\xi_{,\nu} - \frac{1}{2}g_{\mu\nu}\xi^{,\rho}\xi_{,\rho} \right) \quad (10)$$

$$T_{\mu\nu}^{\text{matter}} \rightarrow \frac{1}{\phi} T_{\mu\nu}^{\text{matter}} \quad (11)$$

$$\square\xi = -4\pi\lambda e^{-\xi}\psi^{,\mu}\psi_{,\mu} \quad (12)$$

$$\square\psi = \psi^{,\mu}\xi_{,\mu}. \quad (13)$$

We define auxiliary variables in terms of the derivatives of the scalar fields

$$\Phi_{\xi} \equiv \frac{\partial}{\partial r}\xi \quad \text{and} \quad \Pi_{\xi} \equiv \frac{a}{\alpha} \frac{\partial}{\partial t}\xi \quad (14)$$

$$\Phi_{\psi} \equiv \frac{\partial}{\partial r}\psi \quad \text{and} \quad \Pi_{\psi} \equiv \frac{a}{\alpha} \frac{\partial}{\partial t}\psi \quad (15)$$

so that the wave equations result in

$$\begin{aligned} \dot{\Phi}_{\xi} &= \left(\frac{\alpha}{a} \Pi_{\xi} \right)' \\ \ddot{\Pi}_{\xi} &= \frac{1}{r^2} \left(\frac{r^2\alpha}{a} \Phi_{\xi} \right)' + 4\pi\lambda e^{-\xi} \frac{\alpha}{a} (\Phi_{\psi}^2 - \Pi_{\psi}^2) \end{aligned} \quad (16)$$

$$\begin{aligned} \dot{\Phi}_{\psi} &= \left(\frac{\alpha}{a} \Pi_{\psi} \right)' \\ \ddot{\Pi}_{\psi} &= \frac{1}{r^2} \left(\frac{r^2\alpha}{a} \Phi_{\psi} \right)' + \frac{\alpha}{a} (\Pi_{\psi}\Pi_{\xi} - \Phi_{\psi}\Phi_{\xi}). \end{aligned}$$

The only other necessary conditions come from the field equations, which, in the Einstein frame, are simply Einstein's field equations, $G_{\mu\nu} = 8\pi T_{\mu\nu}$. In accordance with the 3+1 formalism, we have the Hamiltonian constraint

$$a' = -\frac{a^3 - a}{2r} + 2\pi ar \left(e^{-\xi} (\Phi_{\psi}^2 + \Pi_{\psi}^2) + \frac{1}{8\pi\lambda} (\Phi_{\xi}^2 + \Pi_{\xi}^2) \right) \quad (17)$$

and the polar slicing condition

$$\alpha' = - \left(\frac{1-a^2}{r} - \frac{a'}{a} \right) \alpha, \quad (18)$$

which enable us to solve for the geometry in terms of the two sources, ψ and ξ . These equations suffice to evolve both the fields $\psi(r, t)$ and $\xi(r, t)$, and the geometric variables $\alpha(r, t)$ and $a(r, t)$ [7].

To show that the model found in [2] is a special case of our model, we compare our Lagrangian

$$L^{\text{BD}} = -\frac{1}{2}e^{-\xi}\psi^{,\rho}\psi_{,\rho} - \frac{1}{16\pi\lambda}\xi^{,\rho}\xi_{,\rho} \quad (19)$$

with that of [2]

$$L^{\tau} = -\frac{1}{32\pi} (e^{4\phi} a_{,\mu} a^{,\mu} + 4\phi_{,\mu} \phi^{,\mu}), \quad (20)$$

defined in terms of the axion, a , and the dilaton, ϕ . Comparing Eqs. (19) and (20), we see a correspondence between the two models with a trivial rescaling of the fields

$$\xi = -4\phi \quad \psi = \frac{1}{\sqrt{16\pi}}a \quad \lambda = 8. \quad (21)$$

We have found the critical solutions for a variety of initial data. Specifically, we input the initial configuration of the two fields, and specify the value of λ . The space of initial configurations is schematically represented in Fig. 1.

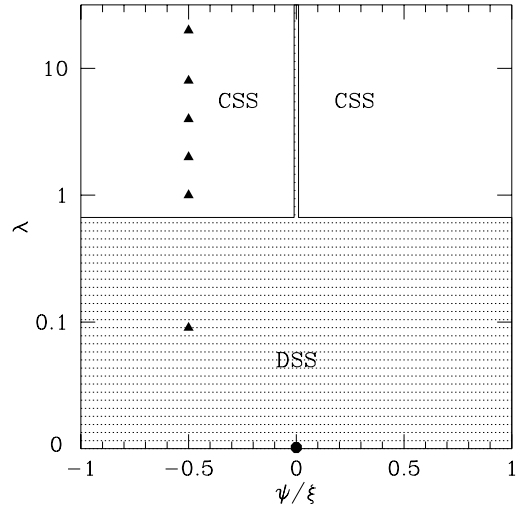


FIG. 1. Schematic of the configuration space. The horizontal axis represents the mixing ratio between the free scalar field and the Brans-Dicke field. The darkened triangles represent the locations of the profiles displayed in Fig. 2. The darkened circle represents the location of the real scalar field in general relativity studied in [1]. For $\lambda < 2/3$, only the DSS solution is the attractor. Above $\lambda \approx 2/3$ the CSS solution attracts whenever both fields are initially present.

We observe for an initially vanishing scalar field that Eqs. (16, 17, 18) describe the real scalar field case studied in [1]. Consistent with this observation, our results recover the same DSS solution found for the real scalar field case. The equivalence between this model with $\psi(r, t) = 0$ and that of the real scalar field is shown in Fig. 1 as the vertical line extending through the middle of the graph.

When $\lambda \rightarrow 0+$, Weinberg shows that the Brans-Dicke model goes over to general relativity. Hence, for the general situation in which both fields are present ($\psi/\xi \neq 0$), we expect to recover the results from general relativity. We do recover the general relativity result, that being the DSS solution. As shown in Fig. 1, the critical solution is discrete for generic initial data as λ is increased up to $\lambda \approx 2/3$.

Shown in Fig. 2 for $\lambda = 0.09$, we have verified that this is the same DSS solution obtained for the real scalar field in general relativity [1]. In Table I, we show the computed values of the echoing exponent Δ . These values correspond to that found in [1].

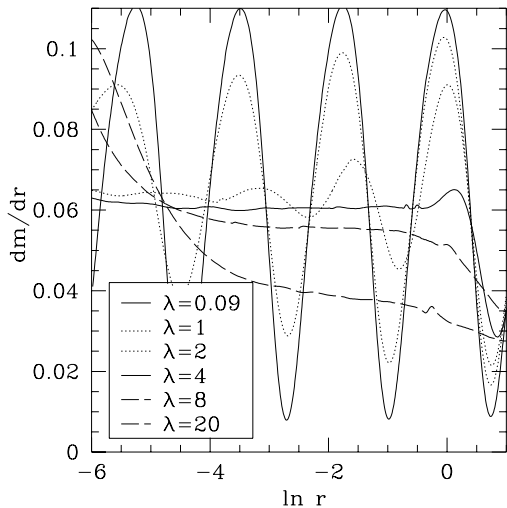


FIG. 2. Demonstration of regime in which the solution transitions from the DSS to the CSS. We show here the mid-section of the seven solutions for various λ . For $\lambda = 0.09$ the solution is clearly the DSS, however the next solution demonstrates that the echoes get damped as one moves towards the origin. Eventually the solutions become the CSS.

Around $\lambda \approx 2/3$, a remarkable transition occurs in the critical solution. As one increases λ in this region, the echos displayed by the critical solution are damped by a decreasing envelope as shown in Fig. 2.

At $\lambda = 8$, we recover, as expected from Eq. (21), the CSS solution found in [2]. In Fig. 3 we demonstrate that the solution found by [2] by demanding continuous self-similarity is indeed the attracting critical solution. Here we show that by a trivial rescaling of the fields at one time slice, our solution is identical to theirs.

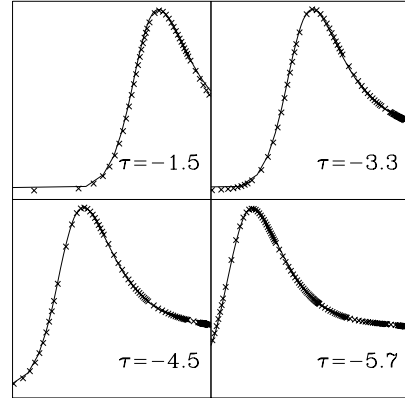


FIG. 3. Demonstration of equivalence between the CSS solution obtained from [2] and our critical solution obtained with $\lambda = 8$. The solid line shows the metric function $a(r, t)$ versus $\ln r$ provided by Eardley. The crosses denote data points from our solution. Four time profiles are shown with $\tau = \ln(T - T^*)$, where T is the central proper time of the slice and T^* is the critical time of collapse. The Eardley and Hirschmann solution is scaled to match our profile at $\tau = -3.3$. The congruence at other times displays the equivalence of the two solutions.

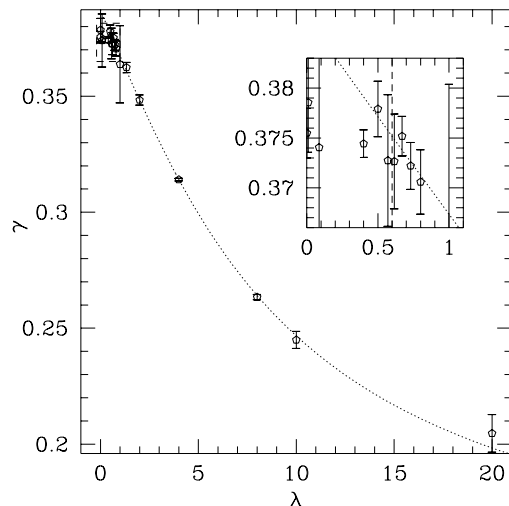


FIG. 4. Black hole mass scaling exponents for various λ . The dotted line displays the values obtained for the non-linear sigma model in [4]. The open pentagons represent the scaling exponent obtained by least-squares fits using our numerical results. The errorbars represent a range of three standard deviations.

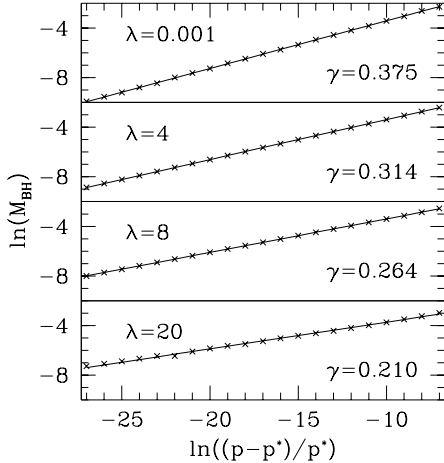


FIG. 5. Illustration of the power-law mass scaling relation. The markers display the mass obtained for the normalized distance from criticality. The lines designate the least-squares fit line with slope γ .

Both the critical solutions exhibit mass-scaling in the supercritical regime. Specifically, for some family of solutions where p^* represents the critical value of a parameter, the masses of the black holes formed in the regime where $p > p^*$ follow

$$M_{\text{BH}} = c(p - p^*)^\gamma \quad (22)$$

where γ depends on λ and c is a family dependent constant. Fig. 5 shows four power law fits and the associated γ 's.

In keeping with the correspondence between this model for very small λ and that of general relativity, we find $\gamma = 0.37$, matching that found in [1]. Likewise, we find agreement between our values of γ and those found by perturbation analysis in [4]. We display both these sets of values in Fig. 4.

The appearance of these two disparate solutions leads one to examine the transition in λ -space from the DSS to the CSS. Bracketing solutions have shown that around $\lambda = 2/3$ the transition occurs (see Fig. 2). As λ is increased around this transition value, an envelope dampens the discrete echos into the smoothly continuous self-similar solution. Perturbation results in the non-linear sigma model confirm a change in stability of the CSS solution near $\lambda = 2/3$ [4].

Further parameter surveys are needed to further specify the transition point between the two self-similar solutions. We also anticipate interesting *negative mass* solutions for $\lambda < 0$. However, our studies have clearly shown the richness of the solution space for even a simple, two-scalar field, one-dimensional problem such as this one.

We are grateful to Douglas Eardley and Eric Hirschmann for discussions and providing us their data. NSF Grants PHY9310083 and PHY9318152 helped support

this research, along with a Cray Research Grant. Computations were performed on the facilities at the Center for High Performance Computing at the University of Texas System.

-
- [1] M. W. Choptuik, Phys. Rev. Lett, **70**, 9-12 (1993).
 - [2] D. Eardley, E. Hirschmann and J. Horne, Phys. Rev. **D52**, 5397-5401 (1995).
 - [3] M. W. Choptuik, T. Chmaj, and P. Bizoń. LANL preprint gr-qc/9603051 (1996).
 - [4] E. W. Hirschmann and D. M. Eardley, LANL preprint gr-qc/9511052 (1995).
 - [5] C. Brans and R. H. Dicke, Phys. Rev. **124**, 925-35 (1961).
 - [6] S. Weinberg, *Gravitation and Cosmology*, (Wiley, New York, 1972).
 - [7] S. L. Liebling, "Massless Scalar Field Collapse In Brans-Dicke Theory", M. A. Thesis, The University of Texas at Austin (unpublished) (1995).

TABLE I. Mass scaling exponents γ and the spatial scaling exponents Δ for the various discretely self-similar solutions found.

λ	ω	γ	Δ
0.001	1000	0.375	
0.01	100	0.379	
0.087	10	0.374	
0.4	1.0	0.374	
0.5	0.5	0.378	
0.57	0.25	0.373	3.447
0.615	0.125	0.373	
0.67	0.0	0.375	3.447
0.73	-0.125	0.372	
0.8	-0.25	0.371	
1.0	-0.50	0.364	
1.33	-0.75	0.362	
2.0	-1.00	0.348	
4.0	-1.25	0.314	
8.0	-1.375	0.263	
10	-1.40	0.245	
20	-1.45	0.205	